Linear dispersive pre-defined peak amplitude modulation of spectrally modulated Airy-based pulses

Miguel A. Preciado[*]

Aston Institute of Photonic Technologies, Aston University, Birmingham, B4 7ET, UK

[*]*m.preciado@aston.ac.uk*

Abstract: Spectrally modulated Airy-based pulses peak amplitude modulation (PAM) in linear dispersive media is investigated, designed, and numerically simulated. As it is shown here, it is possible to design the spectral modulation of the initial Airy-based pulses to obtain a pre-defined PAM profile as the pulse propagates. Although optical pulses self-amplitude modulation is a well-known effect under non-linear propagation, the designed Airy-based pulses exhibit PAM under linear dispersive propagation. This extraordinary linear propagation property can be applied in many kinds of dispersive media, enabling its use in a broad range of experiments and applications.

References and links

1. M. Berry and N. Balazs, "Nonspreading wave packets," Am. J. Phys **47**, 264–267 (1979).
2. G. A. Siviloglou and D. N. Christodoulides, "Accelerating finite energy airy beams," Opt. Lett. **32**, 979–981 (2007).
3. G. Siviloglou, J. Broky, A. Dogariu, and D. Christodoulides, "Observation of accelerating airy beams," Phys. Rev. Lett. **99**, 213901 (2007).
4. I. Kaminer, M. Segev, and D. N. Christodoulides, "Self-accelerating self-trapped optical beams," Phys. Rev. Lett. **106**, 213903 (2011).
5. A. Lotti, D. Faccio, A. Couairon, D. Papazoglou, P. Panagiotopoulos, D. Abdollahpour, and S. Tzortzakis, "Stationary nonlinear airy beams," Physical Review A **84**, 021807 (2011).
6. A. Chong, W. H. Renninger, D. N. Christodoulides, and F. W. Wise, "Airy–bessel wave packets as versatile linear light bullets," Nat. Photonics **4**, 103–106 (2010).
7. D. Abdollahpour, S. Suntsov, D. G. Papazoglou, and S. Tzortzakis, "Spatiotemporal airy light bullets in the linear and nonlinear regimes," Phys. Rev. Lett. **105**, 253901 (2010).
8. Y. Fattal, A. Rudnick, and D. M. Marom, "Soliton shedding from airy pulses in kerr media," Opt. Express **19**, 17298–17307 (2011).
9. A. Rudnick and D. M. Marom, "Airy-soliton interactions in kerr media," Opt. Express **19**, 25570–25582 (2011).
10. C. Ament, P. Polynkin, and J. V. Moloney, "Supercontinuum generation with femtosecond self-healing airy pulses," Phys. Rev. Lett. **107**, 243901 (2011).
11. Y. Hu, M. Li, D. Bongiovanni, M. Clerici, J. Yao, Z. Chen, J. Azaña, and R. Morandotti, "Spectrum to distance mapping via nonlinear airy pulses," Opt. Lett. **38**, 380–382 (2013).
12. M. A. Preciado and M. A. Muriel, "Metodo y sistema para la transmision de pulsos opticos a traves de medios dispersivos," Spain patent **Es2364935** (2010).
13. M. A. Preciado and M. A. Muriel, "Band-limited airy pulses for invariant propagation in single mode fibers," J. Lightwave Technol. **30**, 3660–3666 (2012).
14. M. A. Preciado and K. Sugden, "Proposal and design of airy-based rocket pulses for invariant propagation in lossy dispersive media," Opt. Lett. **37**, 4970–4972 (2012).

15. Y. S. Kivshar and G. Agrawal, *Optical Solitons: From Fibers to Photonic Crystals* (Academic press, 2003).
16. I. Kaminer, Y. Lumer, M. Segev, and D. N. Christodoulides, "Causality effects on accelerating light pulses," Opt. Express **19**, 23132–23139 (2011).
17. M. Potasek and G. Agrawal, "Self-amplitude-modulation of optical pulses in nonlinear dispersive fibers," Phys. Rev. A. **36**, 3862 (1987).
18. O. Vallee and M. Soares, *Airy Functions and Applications to Physics* (Imperial College, 2004).
19. J. Azaña, "Time-frequency (wigner) analysis of linear and nonlinear pulse propagation in optical fibers," EURASIP J. Appl. Sig. Processing **2005**, 1554–1565 (2005).
20. J. Azaña and M. A. Muriel, "Study of optical pulses-fiber gratings interaction by means of joint time-frequency signal representations," J. Lightwave Technol. **21**, 2931 (2003).
21. ITU-T, *Optical Fibres, Cables and Systems* (ITU, 2009).
22. A. Yariv and P. Yeh, *Photonics: Optical Electronics in Modern Communications (The Oxford Series in Electrical and Computer Engineering)* (Oxford University Press, Inc., 2006).
23. M. Ibsen and R. Feced, "Fiber bragg gratings for pure dispersion-slope compensation," Opt. Lett. **28**, 980–982 (2003).
24. M. A. Preciado, V. Garcia-Munoz, and M. A. Muriel, "Grating design of oppositely chirped fbgs for pulse shaping," IEEE Photon. Technol. Lett. **19**, 435–437 (2007).
25. M. A. Preciado, X. Shu, and K. Sugden, "Proposal and design of phase-modulated fiber gratings in transmission for pulse shaping," Opt. Lett. **38**, 70–72 (2013).
26. A. M. Weiner, S. Enguehard, and B. Hatfield, "Femtosecond optical pulse shaping and processing," Prog. Quantum Electron. **19**, 161–238 (1995).

1. Introduction

Airy solutions of the Schrödinger equation were proposed in 1979 [1] within the context of quantum mechanics. In optics, Airy wave-packets were first introduced in the context of spatial optics Airy beams [2, 3] , and the corresponding non-linear dynamics were presented in [4, 5]. These ideas have also been applied in temporal optics, where the unique propagation properties of temporal Airy-based pulses has been recently investigated in both linear and non-linear media, namely in linear light bullets [6, 7], soliton pulses generation [8], Airy-soliton interaction [9], supercontinuum generation [10], spectrum to distance mapping [11], linear dispersive invariant propagation by flat-topped spectrum Airy-based pulses [12, 13], and linear dispersive attenuation invariant propagation by Airy-based "rocket" pulses [14]. In a similar way to optical solitons [15], optical Airy pulses exhibit temporal propagation invariance of the temporal intensity as it propagates through a linear dispersive media during a limited propagation path, until a "critical point" where the pulse breaks up [16]. However, while solitons invariant propagation is due to non-linear effects of the medium, Airy-based pulses invariant propagation is based on linear effects.

Here, the properties of peak amplitude modulation (PAM) of spectrally modulated Airy-based pulses in linear dispersive medium are analysed, designed, and numerically simulated. In non-linear dispersive media, self-amplitude modulation [17] is a well known effect, where the amplitude of the pulse is modulated as it propagates due to both non-linear effects and dispersion. However, only linear effects are involved in the PAM effect of the proposed Airy-based pulses. Moreover, the PAM profile can be pre-defined with some degree of accuracy by applying the proposed design process. As it is illustrated in Fig. 1, the pulse peak intensity is modulated as it propagates through a linear dispersive medium following a pre-defined profile (oscillatory profile example shown in the figure).

In the reminder of this Letter, the theoretical basis of the customizable linear dispersive PAM of the proposed Airy-based pulses is shown. In the examples, several spectrally modulated Airy-based pulses are designed and numerically simulated to obtain 4 pre-defined PAM profiles. Finally, the work is summarized and concluded.
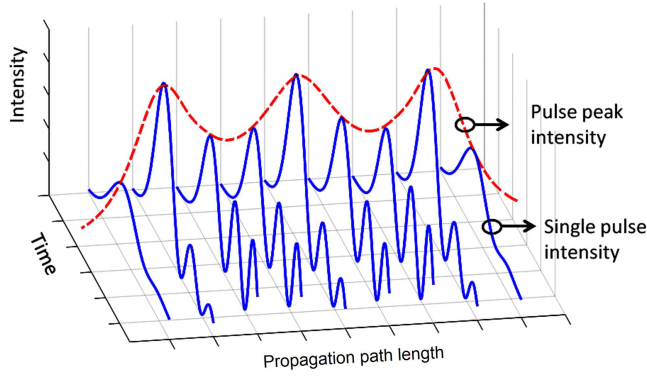
Fig. 1. Illustrative representation of the linear dispersive PAM of the Airy-based pulse (example of oscillatory pre-defined PAM). The propagation delay is not represented for a clear visualization of the PAM.

2. Principle

The chromatic dispersion effect of a linear dispersive media section with length z can be modelled as a phase-only filter $H_D(\omega,z) = exp(-j\beta(\omega)z)$, where ω is the base-band angular frequency, i.e., $\omega = \omega_{opt} - \omega_0$, ω_{opt} is the optical angular frequency, ω_0 is the central angular frequency, j is the imaginary unit, and $\beta(\omega)$ is the propagation constant as a function of ω. $\beta(\omega)$ can be approximated as a Taylor expansion until the second order of ω, $\beta(\omega) = \beta_0 + \beta_1\omega + \beta_2\omega^2/2$, where $\beta_i = d^i\beta(\omega)/d\omega^i$ at $\omega = 0$. An ideal Airy pulse propagated through a dispersive medium can be expressed [13]:

$$F_{prop}(\omega,z) = A(\omega)H_D(\omega,z) = A(\omega - \Delta\omega(z))exp(-j(\Delta t(z)\omega + \phi(z))) \tag{1}$$

where $A(\omega) = exp(j\xi\omega^3)$ represents the Airy pulse in the spectral domain [18], with ξ is a real constant number, $F_{prop}(\omega,z)$ represents the spectral function of the propagated pulse as a function of z, $\phi(z) = \beta_0 z - \xi\left(\frac{\beta_2 z}{6\xi}\right)^3$ represents an added constant phase term [13], $\Delta t(z) = 3\xi\Delta\omega(z)^2 + \beta_1 z$ represents a temporal shift due to the propagation delay [13], and:

$$\Delta\omega(z) = \frac{\beta_2 z}{6\xi} \tag{2}$$

represents a dispersive spectral shift [13] of the Airy pulse.

The proposed spectrally modulated Airy-based pulse can be expressed as:

$$A_M(\omega) = M(\omega)A(\omega) = M(\omega)exp(j\xi\omega^3) \tag{3}$$

, where $M(\omega)$ is a spectral modulation term that must be designed to obtain a pre-defined PAM profile. Using Eq. (1), we can deduce the effect of propagation in a lossy dispersive medium section with length z:

$$\begin{aligned}
F_{M,prop}(\omega,z) &= A_M(\omega)H_D(\omega,z)H_A(\omega,z) = \\
&= M(\omega)A(\omega)H_D(\omega,z)H_A(\omega,z) = \\
&= M(\omega)H_A(\omega,z)A(\omega - \Delta\omega(z))e^{-j(\Delta t(z)\omega + \phi(z))}
\end{aligned} \tag{4}$$

where $H_A(\omega,z)$ represents the transfer function of the losses of the medium section with length z.

Joint time-frequency representations constitute as a very useful method to analyse and visualize the effect of optical pulses propagation in different kinds of optical media [13, 19, 20], where the temporal distribution of the spectral components of optical signal are represented in 2D. Note that these spectral components do not refer to spatial frequencies, but to the frequency components of the temporal waveform. In [13], it was shown that the Airy-based pulses parabolic time-frequency distribution remains invariant, and it is only affected by a simultaneous time-frequency shift, $\Delta t(z)$, $\Delta \omega(z)$, of the whole time-frequency distribution. As it is illustrated in the time-frequency distribution shown in Fig. 2, the spectral components corresponding to the main lobe of the Airy-based pulse are centred at $\Delta \omega(z)$. In temporal domain, the main lobe pulse has a full width half maximum (FWHM) that can be numerically calculated as $FWHM_t = \left| 2.35 \xi^{1/3} \right|$. From this, we can approach the main lobe spectral width, δ_ω, as the corresponding spectral full width half maximum (FWHM) of the main lobe:

$$\delta_\omega \cong FWHM_\omega = 4\log(2)/FWHM_t = \left| 1.2 \xi^{-1/3} \right| \tag{5}$$

where $FWMH_\omega$ is approached as the spectral FWHM of a Gaussian function with same $FWHM_t$ as the main lobe. By using the Parseval theorem, we can approximate the energy of the main lobe of the propagated pulse at z, $E_{ml}(z)$, considering the energy spectral density of the propagated pulse $\left| F_{M,prop}(\omega,z) \right|^2 = \left| M(\omega) H_A(\omega,z) \right|^2$, and the integration interval defined by the main lobe spectral range $\left| \omega - \Delta \omega(z) \right| < \delta_\omega/2$:

$$\begin{aligned}
E_{ml}(z) &\approx \int_{\Delta\omega(z)-\frac{\delta_\omega}{2}}^{\Delta\omega(z)+\frac{\delta_\omega}{2}} \left| F_{M,prop}(\omega,z) \right|^2 \mathrm{d}\omega = \\
&= \int_{\frac{\delta_\omega}{2}}^{\frac{\delta_\omega}{2}} \left| F_{M,prop}(\omega + \Delta\omega(z),z) \right|^2 \mathrm{d}\omega \approx \\
&\approx \delta_\omega \left| F_{M,prop}(\Delta\omega(z),z) \right|^2 = \delta_\omega SAM(z)
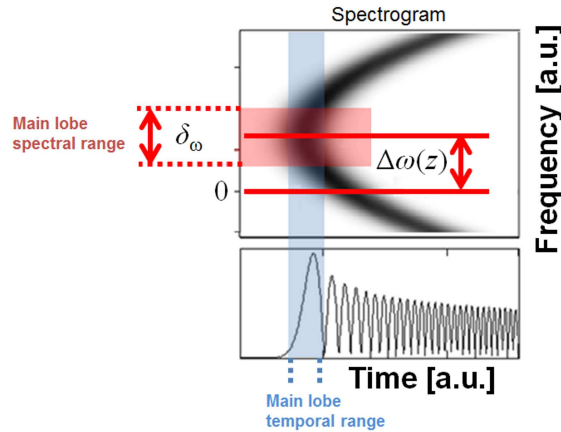\end{aligned} \tag{6}$$

where:

Fig. 2. Time-frequency range of the main lobe of the Airy-based pulse, temporally centred at $t = \Delta t(z)$ within a temporal width $FWHM_t$, and spectrally centred at $\omega = \Delta \omega(z)$ within a spectral width δ_ω. This spectral range is the integration interval used to approximate the main lobe intensity peak by applying the Parseval theorem.

$$PAM(z) = |F_{M,prop}(\Delta\omega(z),z)|^2 = |M(\Delta\omega(z))H_A(\Delta\omega(z),z)|^2 \tag{7}$$

, and we have approached $\left|F_{M,prop}(\omega+\Delta\omega(z),z)\right|^2 \approx \left|F_{M,prop}(\Delta\omega(z),z)\right|^2$ in the interval $|\omega| < \delta_\omega/2$, which will be more accurate providing the the total integration interval range δ_ω is small enough , or equivalently from Eq. (5), ξ is big enough. Since the main lobe peak intensity is proportional to the main lobe total energy, we can deduce:

$$I_{ml}(z) \propto E_{ml}(z) \approx \delta_\omega PAM(z) \tag{8}$$

where $I_{ml}(z)$ denotes the peak intensity of the main lobe. Equation (8) implies that the peak exhibits a PAM effect as it propagates, approximately proportional to $PAM(z)$. From Eq. (7), using a change of variable $\Delta\omega(z) \to \omega$, we can deduce:

$$M(\omega) = \frac{\sqrt{PAM\left(z = \frac{6\omega\xi}{\beta_2}\right)}}{\left|H_A\left(\omega, z = \frac{6\omega\xi}{\beta_2}\right)\right|} \tag{9}$$

where $PAM(z)$ must be real and positive. Assuming a limited z interval of length L, Eq. (9) defines $M(\omega)$ in a limited bandwidth:

$$B = \left|\frac{\beta_2 L}{6\xi}\right| \tag{10}$$

, which from Eq. (3) can also be deduced as the bandwidth of the Airy-based pulse $A_M(\omega)$.

3. Examples and results

In order to illustrate the customizable dispersive linear PAM effect of the proposed Airy-based pulse, several examples are designed and numerically simulated. Without loss of generality, in these examples we consider a linear dispersive medium consisting in a standard single mode fibre and ITU-T G.652 specifications, which dispersion parameter can be modelled as $\beta_2 = -21.68\,ps^2/km$ at the central frequency $\omega_0 = 2\pi f_0$ with f_0=193.413 THz (1550 nm wavelength). In these example we consider a path length of L=10 km, where the origin of z is set in the middle of the propagation path, i.e., $z \in [-L/2, L/2]$. The attenuation parameter is modelled as $\alpha(\omega) = \alpha_0 + \alpha_1\omega$ dB/km, with α_0=0.2 dB/km, and α_1=0.45 fs dB/km, values obtained from typical values in Table 1.2 of [21].

The attenuation transfer function at a fibre position z can be expressed:

$$H_A(z,\omega) = 10^{-\frac{\alpha(\omega)(z+L/2)}{20}} \tag{11}$$

In these examples, we assume four customized $PAM(z)$ profile functions shown in Fig. 3. The resulting spectral functions of the Airy-based pulses can be obtained from Eqs. (3) and (9) as:

$$A_M(\omega) = \sqrt{PAM\left(z = \frac{6\omega\xi}{\beta_2}\right)}\, 10^{\frac{\alpha(\omega)}{20}\left(\frac{6\omega\xi}{\beta_2}+\frac{L}{2}\right)} e^{j\xi\omega^3} \tag{12}$$

where the resulting spectral function depends on the value of ξ. In order to facilitate the design process, it is practical to have ξ expressed as a function of a normalized parameter $r = \frac{\delta_\omega}{B}$, which represents the pulse main lobe bandwidth to full pulse bandwidth ratio. Using Eq. (10) we can deduce $\delta_\omega = rB = \frac{r\beta_2 L}{6\xi}$, and from Eq. (5) we can obtain:
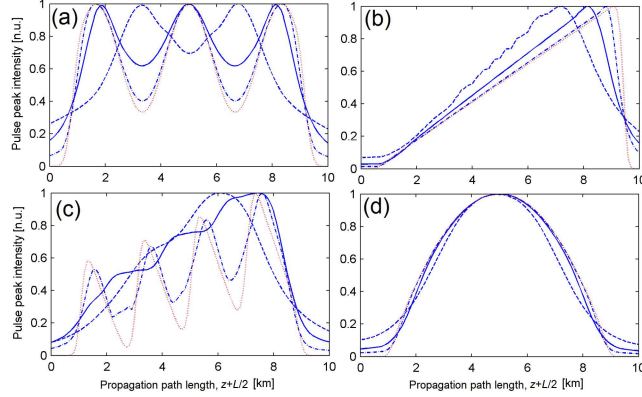
Fig. 3. Four pre-defined $PAM(z)$ profiles (red-dotted), and the numerically obtained propagated pulse peak intensity, using $r = 0.2$ (blue-dashed), $r = 0.1$ (blue-solid), and $r = 0.05$ (blue-dash-dotted), for examples from (a) to (d), in a propagation path of L=10 km.
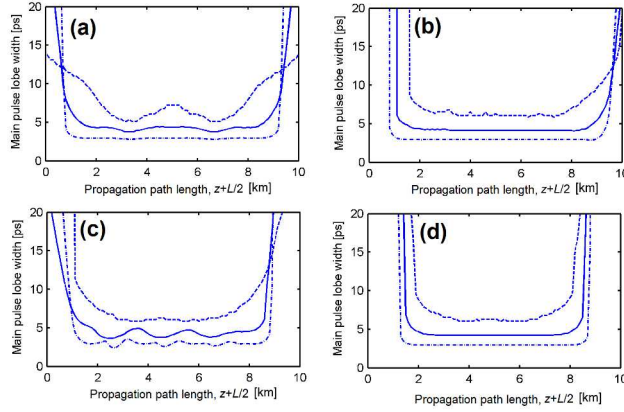

Fig. 4. Main lobe temporal width of the Airy-based pulse for examples from (a) to (d), using $r = 0.2$ (blue-dashed), $r = 0.1$ (blue-solid), and $r = 0.05$ (blue-dash-dotted), in a propagation path of L=10 km.

$$|\xi| = \left| \frac{\beta_2 L r}{7.2} \right|^{\frac{3}{2}}$$ (13)

The temporal waveform of the resulting propagated pulse at a position z of the propagation path can be obtained from $f_{M,prop}(t,z) = IFT[F_{M,prop}(\omega,z)]$, where IFT denotes the inverse Fourier transform, and $F_{M,prop}(\omega,z)$ can be calculated from 4. Figure 3 represents the evolution of the peak intensity of the propagated pulse through a path of L =10 km for r= 0.2, 0.1 and 0.05, with ξ= -14.779, -5.225, and -1.847 ps^3 from Eq. (13), and$(B/2\pi)$=0.19, 0.55 and 1.55 THz from Eq. (10). As it can be observed, the agreement between the actual PAM of the pulse peak intensity and the pre-defined $PAM(z)$ function improves as r decreases, or equivalently, ξ increases. Although in the previous analysis we have considered the main lobe of the Airy-based pulse with an approximately constant temporal width as the pulse propagates, the spectral modulation will unavoidable affect to the main lobe width. Figure 4 shows the evolution of the
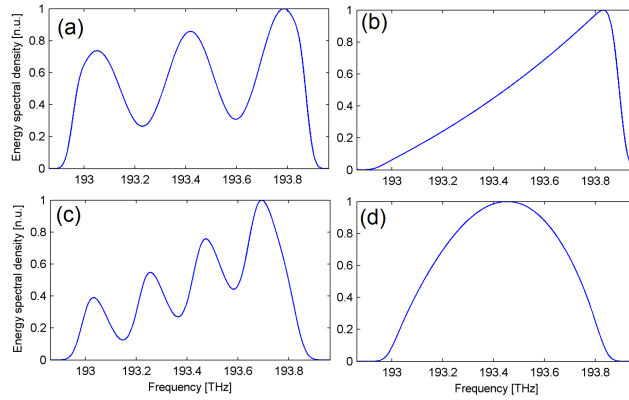
Fig. 5. Energy spectral density $|A_M(z)|^2 = |M(z)|^2$ of the Airy-based pulse for examples from (a) to (d), for $r = 0.1$.
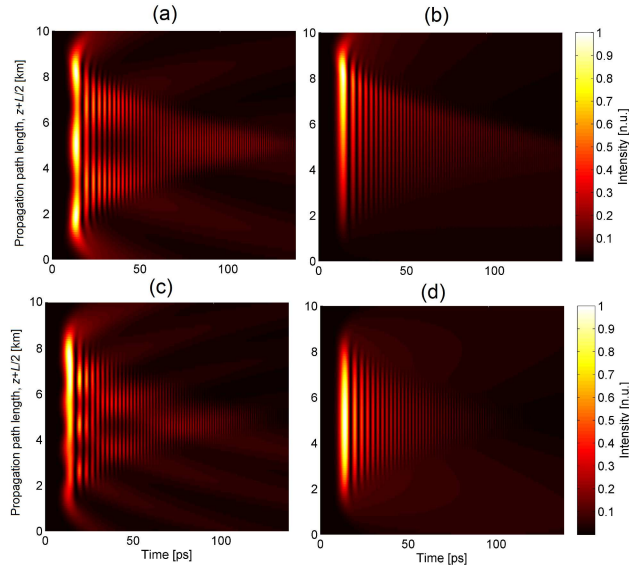

Fig. 6. Color map representation of the evolution of the temporal intensity of the propagated Airy-based pulse for examples from (a) to (d), in a propagation path of $L=10$ km.The propagation delay is not represented for a clear visualization of the PAM.

temporal width of the main lobe in the pulse propagation path, where the effect of the spectral modulation can be observed. Again, lower r values improve the approximation accuracy, obtaining a more uniform temporal width evolution.

The selection of the value of the design variable r involves a trade-off solution between the pre-defined PAM profile complexity, the usable bandwidth, and the desired PAM profile accuracy, according to the specifications of a particular application. Let us focus here on the case $r = 0.1$, where a reasonable PAM accuracy is obtained for the four pre-defined PAM profiles (see Fig. 3). Figure 5 shows the corresponding spectral functions, and Fig. 6 represents the pulse waveform through a propagation path of $L=10$ km, where the propagation delay has been

neglected for a clear visualization of the linear dispersive PAM effect. As it can be observed, the main lobe peak intensity of the Airy-based pulses exhibits a linear dispersive PAM corresponding to the $PAM(z)$ profile functions.

It is worth noting that the third order dispersion parameter $\beta_3 = d^3\beta(\omega)/d\omega^3$ has not been considered in the design process, having a marginal effect in the previous examples. The effect of third order dispersion can be neglected provided the quasi-non-distortion condition proposed in [13], $|\beta_3 L/12| \ll |\xi|$, is satisfied. For this particular case, an ITU-T G.652 standard single mode fibre has a typical value $\beta_3 = 0.0911 ps^3/km$, leading to a condition $|\xi| \gg 0.0756 ps^3$, satisfied in the previous examples. If the quasi-non-distortion condition is not satisfied, third-order dispersion cannot be neglected, and will affect distorting the resulting PAM profile. In that case, further analyses must be done in order to deduce additional considerations in the design process to compensate the third-order dispersion induced PAM distortion.

4. Conclusion

In summary, linear dispersive PAM effect of the proposed spectrally modulated Airy-based pulses has been analysed, designed, and numerically demonstrated. As it is shown in the examples, the initial Airy-based pulses can be designed to exhibit a pre-defined PAM profile as it propagates through the linear dispersive medium.

The main limitation of the proposed technique consists in the PAM distortion due to too high r value (or equivalently, insufficient bandwidth), as well as the third order dispersion in case the quasi-non-distortion condition [13] is not satisfied. However, this PAM distortion can be probably mitigated in the design process, which would require deeper study and analysis of the pulse propagation in these conditions, out of the scope of the present work.

In order to emphasize the unique properties of the designed Airy based pulses, we can compare these results with a trivial case, considering a transform-limited Gaussian pulses with an initial temporal width (FWHM) equal to w_g. It can be deduced that the pulse PAM in this case can be expressed as [22] $PAM_g(z) = 1/\sqrt{1+pz^2}$ with $p = 4\beta_2 \ln 2/w_g^2$. As it can be observed, the set of possible PAM profiles is very restricted, and only depends on the value p. However, applying spectrally modulated Airy-based pulses with the design principles presented here, we can obtain diverse pre-defined PAM profiles along the z axis.

Different pulse shaping techniques can be applied to generate the initial Airy-based pulse $A_M(\omega)$ from a pulsed laser source. Spatial light modulators [26] have been successfully applied for generating Airy-based pulses in [10], by spectral manipulation of the spectral components of the optical signal. Also, fiber Bragg gratings have shown to be useful in shaping optical pulses of relative complexity [23–25].

It is worth noting that, although the examples have been designed considering an optical fibre, any linear dispersive medium can be considered, providing the chromatic dispersion is the dominant term, resulting in a broad range of experiments and applications exploiting this unique linear propagation property.